

# Electrostatics in the presence of spherical dielectric discontinuities

Cite as: J. Chem. Phys. **128**, 214505 (2008); <https://doi.org/10.1063/1.2908077>

Submitted: 07 January 2008 . Accepted: 21 March 2008 . Published Online: 03 June 2008

Per Linse



View Online



Export Citation

## ARTICLES YOU MAY BE INTERESTED IN

[Electrostatic analysis of the interactions between charged particles of dielectric materials](#)

The Journal of Chemical Physics **133**, 024105 (2010); <https://doi.org/10.1063/1.3457157>

[Image charges in spherical geometry: Application to colloidal systems](#)

The Journal of Chemical Physics **117**, 11062 (2002); <https://doi.org/10.1063/1.1521935>

[Green's function for a spherical dielectric discontinuity and its application to simulation](#)

The Journal of Chemical Physics **140**, 044903 (2014); <https://doi.org/10.1063/1.4862148>

## Lock-in Amplifiers up to 600 MHz

starting at

\$6,210



Zurich  
Instruments

Watch the Video



# Electrostatics in the presence of spherical dielectric discontinuities

Per Linse<sup>a)</sup>*Physical Chemistry 1, Center for Chemistry and Chemical Engineering, Lund University, P. O. Box 124, SE-221 00 Lund, Sweden*

(Received 7 January 2008; accepted 21 March 2008; published online 3 June 2008)

A united description of the electrostatics of an arbitrary number of electrostatic multipoles, each localized in a spherical dielectric cavity, in a dielectric medium is presented. The permanent charges as well as the polarization surface charges are described by multipole expansions in standard format. Expressions of the polarization surface charge density, the electrostatic potential energy, and the electrostatic interaction including the contribution from the polarization surface charge densities are given. Interacting electrostatic multipoles in dielectric spheres immersed in a medium with a higher (lower) relative dielectric permittivity experience a repulsive (attractive) potential term that increases in magnitude at reduced multipole separation, originating from the polarization surface charges appearing at the dielectric interfaces. Simplified expressions applied to monopoles and to two dielectric cavities are provided. Numerical examples involving monopoles and dipoles quantifying the effect of the surface polarization are also included. © 2008 American Institute of Physics. [DOI: 10.1063/1.2908077]

## I. INTRODUCTION

Even on the classical level of description, condensed matter such as charged species dissolved in a solution possesses several intellectual challenges. One of the most remarkable approximations is the so-called dielectric approximation applied to solutions of ionic species.<sup>1-3</sup> This approximation involves a replacement of a model system composed of charged species and solvent with a gas of the charged species, now with their interaction attenuated by the relative dielectric permittivity of the solvent. This simplification applied to arbitrary solutes is sometimes referred to as the McMillan–Mayer theory.<sup>4</sup>

An astonishing finding is that the dielectric approximation holds for simple ions dissolved in water down to only a few layers of water between the ions.<sup>5-7</sup> This success of the dielectric approximation lies behind the usefulness of the Poisson–Boltzman (PB) equation applied to aqueous solutions of monovalent ions. However, for multivalent ions the PB equation becomes less accurate; an observation that is attributed to the neglect of the ion-ion correlations in the PB theory.<sup>8</sup>

The dielectric approximation is also ubiquitous when describing charged colloids in aqueous solutions; here colloids refer to proteins, silica particles, latex particles, etc.<sup>9-13</sup> In most cases, the different dielectric permittivity of the colloids and the solvent is neglected, mainly for the technical complexity to include it.

A charge in a dielectric medium polarizes the medium.<sup>1,2</sup> Consequently, a charge near a boundary between two media with different dielectric properties leads to a polarization surface charge density at the boundary. For a single and planar dielectric discontinuity, the electrostatic potential on either side of the discontinuity arising from the polarization surface

charge is simple to describe<sup>2</sup> and it can be reexpressed as the electrostatic potential arising from a so-called image charge on the other side of the discontinuity. With several and parallel dielectric discontinuities, the induced surface charges have to be solved self-consistently, but the algebra is still relatively simple.

The corresponding expressions for a charge near a spherical dielectric discontinuity have also been provided.<sup>1,14-16</sup> The physical interpretation of the polarization surface charge in terms of image charges becomes less trivial, since each charge gives rise to a manifold of image charges.<sup>15</sup> Furthermore, systems composed of two spherical dielectric cavities with monopoles,<sup>17,18</sup> multipoles, but retaining an overall axial symmetry,<sup>19</sup> or with general multipoles<sup>20</sup> have been examined with multipole expansions. In addition, two spherical dielectric cavities with monopoles have also been analyzed with bispherical coordinates.<sup>21,22</sup> A reduction of these expressions to a single cavity leads to the classical Born model<sup>23</sup> describing the solvation of ions in dielectric media and to the reaction field of a point dipole in a medium.<sup>24,25,1</sup> Variational formulations have also been applied to solve dielectric boundary problems.<sup>26,27</sup>

The present contribution provides a united description of the electrostatic interaction of an arbitrary set of electrostatic multipoles, each localized in a spherical cavity possessing a dielectric permittivity different from that of the surroundings. In the following section, the basic expressions describing electrostatic charge distributions, potentials, and fields in vacuum are provided with special focus on expansions in spherical harmonics. Thereafter, the interaction energies between overlapping and between nonoverlapping charge distributions are discussed using the notation introduced. The relevant equations for describing polarization in media and polarization surface charges at dielectric discontinuities are briefly given in the following section. This is followed by a derivation of general expressions of the polarization surface

<sup>a)</sup>Electronic mail: per.linse@fkem1.lu.se.

charge densities, electrostatic potential energies, and the electrostatic interaction, for a system containing an arbitrary number of electrostatic multipoles, each localized in a spherical dielectric cavity, in a dielectric medium. Thereafter, corresponding expressions for simplified systems involving monopoles and involving two cavities are presented. The contribution ends with some numerical examples quantifying the effect of the surface polarization on the electrostatic interaction. Further application of the present formalism to investigate the potential of mean force between two low-dielectric charged colloids in water will be given in a forthcoming paper.<sup>28</sup>

## II. A SINGLE CHARGE DISTRIBUTION

In vacuum, a charge distribution,  $\rho(\mathbf{r}')$ , in a finite volume,  $V$ , generates an electrostatic potential,  $\phi$ , at a field point,  $\mathbf{r}$ , according to

$$\phi(\mathbf{r}) = \frac{1}{4\pi\epsilon_0} \int_V d\mathbf{r}' \frac{\rho(\mathbf{r}')}{|\mathbf{r} - \mathbf{r}'|}. \quad (1)$$

With the use of an expansion of  $1/|\mathbf{r} - \mathbf{r}'|$  in Racah's unnormalized spherical harmonics  $C_{lm}(\Omega)$ ,  $\Omega \equiv (\theta, \varphi)$  with  $\theta$  and  $\varphi$  denoting the spherical polar angles, according to (see p. 151 of Ref. 29)

$$\frac{1}{|\mathbf{r} - \mathbf{r}'|} = \sum_{lm} \frac{r'^l}{r^{l+1}} C_{lm}^*(\Omega) C_{lm}(\Omega'), \quad (2)$$

where  $r_{<} \equiv \min(r, r')$ ,  $r_{>} \equiv \max(r, r')$ , and  $\sum_{lm} \equiv \sum_{l=0}^{\infty} \sum_{m=-l}^l$ , we get

$$\phi(\mathbf{r}) = \frac{1}{4\pi\epsilon_0} \int_V d\mathbf{r}' \sum_{lm} \frac{r'^l}{r^{l+1}} \rho(\mathbf{r}') C_{lm}^*(\Omega) C_{lm}(\Omega'). \quad (3)$$

Here, and in the following, a star denotes the complex conjugate. Two cases can now be considered: (i) the location of the field point being further away than all charges in the charge distribution,  $\rho$ , from the expansion point ( $r > r'_{\max}$ ) and (ii) The location of the field point being closer than all charges in the charge distribution,  $\rho$ , to the expansion point ( $r < r'_{\min}$ ). In those cases, the electrostatic potential can then be expressed as

$$\phi(\mathbf{r}) = \frac{1}{4\pi\epsilon_0} \sum_{lm} Q_{lm}^> \frac{1}{r^{l+1}} C_{lm}^*(\Omega), \quad r > r'_{\max}, \quad (4)$$

$$\phi(\mathbf{r}) = \frac{1}{4\pi\epsilon_0} \sum_{lm} Q_{lm}^< r^l C_{lm}^*(\Omega), \quad r < r'_{\min}, \quad (4')$$

respectively, where the spherical multipole moments  $Q_{lm}^>$  and  $Q_{lm}^<$  are defined according to

$$Q_{lm}^> \equiv \int_V d\mathbf{r}' \rho(\mathbf{r}') r'^l C_{lm}(\Omega'), \quad r > r'_{\max}, \quad (5)$$

$$Q_{lm}^< \equiv \int_V d\mathbf{r}' \rho(\mathbf{r}') \frac{1}{r'^{l+1}} C_{lm}(\Omega'), \quad r < r'_{\min}. \quad (5')$$

The moments with  $l=0, 1, 2, 3, \dots$  denote monopole (charge), dipole, quadrupole, octupole, etc. The spherical multipole moments  $Q_{lm}$  transfer under rotation as the spherical harmonics. Moreover,

$$Q_{lm}^* = (-1)^m Q_{l,-m}. \quad (6)$$

In addition, if the charge distribution has an inversion center, then  $Q_{lm}=0$  for odd  $l$ . An axial charge distribution has only one independent component for each  $l$ . If the symmetry axis coincides with the azimuthal axis, we have  $Q_{lm}=0$  for  $m \neq 0$ . More generally, for a charge distribution with a  $n$ -fold symmetry axis, we have  $Q_{lm}=0$  for  $m \neq 0$  if  $l < m$ .

Now consider a charge distribution on the spherical surface,  $S$ , with the radius,  $a$ , according to

$$\rho(\mathbf{r}) = \delta(r-a) \sigma(\Omega), \quad (7)$$

where  $\delta$  is the Dirac delta function and  $\sigma(\Omega)$  denotes the surface charge density. Since the spherical harmonics constitute a complete set, the surface charge density can be expanded according to

$$\sigma(\Omega) = \sum_{lm} \frac{2l+1}{4\pi a^2} \sigma_{lm} C_{lm}^*(\Omega), \quad (8)$$

where the expansion coefficients  $\sigma_{lm}$ ,

$$\sigma_{lm} \equiv \int_S d\Omega' \sigma(\Omega') a^2 C_{lm}(\Omega'), \quad (9)$$

are referred to as the spherical surface charge multipole moments. Equations (5), (7), and (9) give the following relation between the spherical multipole moments and the spherical surface charge multipole moments for a spherical surface charge distribution:

$$Q_{lm}^> = a^l \sigma_{lm}, \quad r > a, \quad (10)$$

$$Q_{lm}^< = \frac{1}{a^{l+1}} \sigma_{lm}, \quad r < a. \quad (10')$$

The insertion of Eq. (10) into Eq. (4) shows that the electrostatic potential at  $\mathbf{r}$  with respect to the center of a spherical surface charge density is given by

$$\phi(\mathbf{r}) = \frac{1}{4\pi\epsilon_0} \sum_{lm} \sigma_{lm} \frac{a^l}{r^{l+1}} C_{lm}^*(\Omega), \quad r > a, \quad (11)$$

$$\phi(\mathbf{r}) = \frac{1}{4\pi\epsilon_0} \sum_{lm} \sigma_{lm} \frac{r^l}{a^{l+1}} C_{lm}^*(\Omega), \quad r < a. \quad (11')$$

The electrostatic field,  $\mathbf{E}$ , at the field point,  $\mathbf{r}$ , is related to the electrostatic potential,  $\phi$ , according to

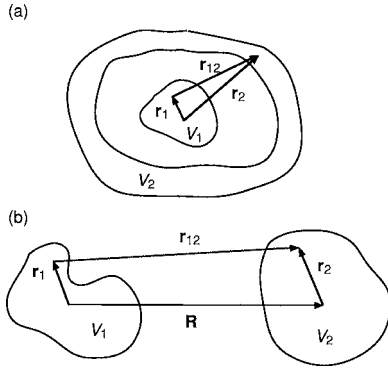


FIG. 1. Illustration of two nonoverlapping charge distributions in the volumes  $V_1$  and  $V_2$ , respectively, where (a)  $V_1$  is enclosed by  $V_2$  and (b)  $V_1$  and  $V_2$  are not enclosing each other.

$$\mathbf{E}(\mathbf{r}) = -\nabla\phi(\mathbf{r}). \quad (12)$$

The electrostatic field in the normal direction from the center of the multipole becomes with help of Eqs. (12) and (4),

$$E_n(\mathbf{r}) = \frac{1}{4\pi\epsilon_0} \sum_{lm} (l+1) Q_{lm}^> \frac{1}{r^{l+2}} C_{lm}^*(\Omega), \quad r > r'_{\max}, \quad (13)$$

$$E_n(\mathbf{r}) = \frac{1}{4\pi\epsilon_0} \sum_{lm} (-l) Q_{lm}^< r^{l-1} C_{lm}^*(\Omega), \quad r < r'_{\min}. \quad (13')$$

### III. TWO NONOVERLAPPING CHARGE DISTRIBUTIONS

We will now consider the two nonoverlapping charge distributions,  $\rho_1$  and  $\rho_2$ , within the volumes,  $V_1$  and  $V_2$ , respectively, in vacuum. From Coulomb's law and the superposition principle, the interaction energy between the two charge distributions becomes

$$U = \frac{1}{4\pi\epsilon_0} \int_{V_1} d\mathbf{r}_1 \int_{V_2} d\mathbf{r}_2 \frac{\rho_1(\mathbf{r}_1)\rho_2(\mathbf{r}_2)}{|\mathbf{r}_2 - \mathbf{r}_1|}. \quad (14)$$

With the electrostatic potential given by Eq. (1), the interaction energy can also be expressed as

$$U = \int_{V_2} \rho_2(\mathbf{r}_2) \phi_1(\mathbf{r}_2) d\mathbf{r}_2, \quad (15)$$

$$U = \int_{V_1} \rho_1(\mathbf{r}_1) \phi_2(\mathbf{r}_1) d\mathbf{r}_1, \quad (15')$$

i.e., the interaction energy can be obtained by integration of  $\rho_2(\mathbf{r}_2)\phi_1(\mathbf{r}_2)$  over the volume  $V_2$ , where  $\phi_1(\mathbf{r}_2)$  is the potential at  $\mathbf{r}_2$  generated by the charge distribution  $\rho_1$ . Obviously, the reverse also holds by symmetry. In the following, we will examine two cases: (i)  $V_1$  being enclosed by  $V_2$  and (ii)  $V_1$  and  $V_2$  not enclosing each other, as illustrated in Fig. 1.

Consider a charge distribution,  $\rho_1(\mathbf{r}_1)$ , within volume,  $V_1$ , and a charge distribution,  $\rho_2(\mathbf{r}_2)$ , within volume,  $V_2$ , where  $\rho_1$  is enclosed by  $\rho_2$  [Fig. 1(a)]. The spherical multipoles  $Q_1$  and  $Q_2$  of the two charge distributions refer to the same expansion center, the origin of the coordinate system. The interaction energy between the two charge distributions

can be reformulated by substituting Eq. (2) with  $\mathbf{r} \rightarrow \mathbf{r}_2$  and  $\mathbf{r}' \rightarrow \mathbf{r}_1$  into Eq. (14) and the subsequent integrations over  $V_1$  and  $V_2$  leading to

$$U = \frac{1}{4\pi\epsilon_0} \sum_{lm} Q_{1,lm} Q_{2,lm}^*, \quad (16)$$

where the spherical multipole moments  $Q_{1,lm} = Q_{lm}^>$  and  $Q_{2,lm} = Q_{lm}^<$  given by Eqs. (5), respectively, have been used.

In the case of nonoverlapping and nonenclosing charge distributions [Fig. 1(b)], the inverse distance  $1/r_{12}$  cannot be expanded according to Eq. (2), since  $\mathbf{r}_1$  and  $\mathbf{r}_2$  originate from different points, viz.  $\mathbf{0}$  and  $\mathbf{R}$ , respectively. Instead, provided that  $|\mathbf{r}_1 - \mathbf{r}_2| < R$ ,  $1/r_{12}$  can be expanded according to

$$\begin{aligned} \frac{1}{r_{12}} &= \frac{1}{|\mathbf{r}_1 - \mathbf{R} + \mathbf{R} + \mathbf{r}_2|} = \frac{1}{|\mathbf{R} - (\mathbf{r}_1 - \mathbf{r}_2)|} \\ &= \sum_{LM} \frac{|\mathbf{r}_1 - \mathbf{r}_2|^L}{R^{L+1}} C_{LM}^*(\Omega) C_{LM}(\Omega'), \end{aligned} \quad (17)$$

where Eq. (2) has been used and with  $\Omega'$  denoting the direction of  $\mathbf{r}_1 - \mathbf{r}_2$  relative to the external coordinate system. With the help of an expansion of  $|\mathbf{r}_1 - \mathbf{r}_2|^L C_{LM}(\Omega')$  in terms of  $r_1$ ,  $\Omega_1$ ,  $r_2$ , and  $\Omega_2$  (see p. 151 of Ref. 29), Eq. (17) can be expressed as

$$\begin{aligned} \frac{1}{r_{12}} &= \sum_{l_1 m_1} \sum_{l_2 m_2} (-1)^{l_1 - M} \left[ \frac{(2L)!}{(2l_1)! (2l_2)!} \right]^{1/2} \sqrt{2L+1} \\ &\times \begin{pmatrix} l_1 & l_2 & L \\ m_1 & m_2 & -M \end{pmatrix} r_1^{l_1} C_{l_1 m_1}(\Omega_1) r_2^{l_2} C_{l_2 m_2}(\Omega_2) \\ &\times \frac{1}{R^{L+1}} C_{LM}^*(\Omega), \end{aligned} \quad (18)$$

with  $L=l_1+l_2$  and  $M=m_1+m_2$ . The phase  $(-1)^{l_1}$  in Eq. (18) originates from the definition that  $\mathbf{R}$  points from charge distribution  $\rho_1$  to  $\rho_2$ . Eventually, the substitution of Eq. (18) into Eq. (14) gives the interaction energy between the two charge distributions. By using the definition of the spherical multipole moments, Eq. (5), we get

$$\begin{aligned} U &= \frac{1}{4\pi\epsilon_0} \sum_{l_1 m_1} \sum_{l_2 m_2} (-1)^{l_1 + M} \left[ \frac{(2L)!}{(2l_1)! (2l_2)!} \right]^{1/2} \sqrt{2L+1} \\ &\times \begin{pmatrix} l_1 & l_2 & L \\ m_1 & m_2 & -M \end{pmatrix} Q_{1,l_1 m_1} Q_{2,l_2 m_2} \frac{1}{R^{L+1}} C_{LM}^*(\Omega). \end{aligned} \quad (19)$$

Equation (19) can be used to obtain the electrostatic potentials. Let  $\phi_1(\mathbf{R} + \mathbf{r}_2)$  denote the electrostatic potential generated by charge distribution  $\rho_1$  at  $\mathbf{R} + \mathbf{r}_2$  and  $\phi_2(\mathbf{r}_1)$  denote the electrostatic potential generated by charge distribution  $\rho_2$  at  $\mathbf{r}_1$ . These potentials are obtained by the insertion of the spherical multipole moments  $Q_{lm}$  according to Eq. (5) into Eq. (19) followed by an identification with Eq. (15) (and the substitution  $\mathbf{r}_2 \rightarrow \mathbf{R} + \mathbf{r}_2$  in the former case), giving

$$\begin{aligned}
\phi_1(\mathbf{R} + \mathbf{r}_2) &= \frac{1}{4\pi\epsilon_0} \sum_{l_1 m_1} \sum_{l_2 m_2} \\
&\times (-1)^{l_1 - M} \left[ \frac{(2L)!}{(2l_1)! (2l_2)!} \right]^{1/2} \sqrt{2L+1} \\
&\times \begin{pmatrix} l_1 & l_2 & L \\ m_1 & m_2 & -M \end{pmatrix} Q_{1,l_1 m_1} r_2^{l_2} C_{l_2 m_2}(\Omega_2) \\
&\times \frac{1}{R^{L+1}} C_{LM}^*(\Omega), \quad (20)
\end{aligned}$$

$$\begin{aligned}
\phi_2(\mathbf{r}_1) &= \frac{1}{4\pi\epsilon_0} \sum_{l_1 m_1} \sum_{l_2 m_2} \\
&\times (-1)^{l_1 + M} \left[ \frac{(2L)!}{(2l_1)! (2l_2)!} \right]^{1/2} \sqrt{2L+1} \\
&\times \begin{pmatrix} l_1 & l_2 & L \\ m_1 & m_2 & -M \end{pmatrix} r_1^{l_1} C_{l_1 m_1}(\Omega_1) \\
&\times Q_{2,l_2 m_2} \frac{1}{R^{L+1}} C_{LM}^*(\Omega). \quad (21)
\end{aligned}$$

#### IV. DIELECTRIC MEDIA AND DISCONTINUITIES

So far, only the electrostatic interaction in vacuum has been examined. However, in the following we will consider charge distributions in microscopically homogeneous media. We impose the restriction that a medium is isotropic, homogeneous, displays linear response, and is polarized only by the homogeneous part of the electrostatic field. In this description, we are interested to determine the polarization surface charge densities at the dielectric discontinuities occurring at the boundaries between different media and the (partly free) electrostatic energy of the system.

An electrostatic field in a medium characterized above gives rise to a polarization dipole density. Therefore, at the boundary between two different media a polarization surface charge density will appear. The electrostatic field equations for continuous media show that the potential across the interface remains continuous, and if the interface does not possess permanent surface charges, the normal component of the dielectric displacement also remains continuous across the interface.<sup>1,2</sup> Thus, that implies

$$\phi_1(\mathbf{r}) = \phi_2(\mathbf{r}), \quad \mathbf{r} \in S, \quad (22)$$

$$\epsilon_1 E_{n_1}(\mathbf{r}) = \epsilon_2 E_{n_2}(\mathbf{r}), \quad \mathbf{r} \in S, \quad (23)$$

where  $\epsilon_1$  and  $\epsilon_2$  are the relative dielectric permittivities of medium 1 and 2, respectively, and  $S$  is the interface between medium 1 and 2. By using  $\epsilon_0 \mathbf{E}(\mathbf{r}) = \epsilon_0 \mathbf{E}(\mathbf{r}) + \mathbf{P}(\mathbf{r})$ , where  $\mathbf{P}(\mathbf{r})$  is the polarization density at  $\mathbf{r}$ , the polarization surface charge density  $\sigma$  at  $\mathbf{r}$  becomes

$$\begin{aligned}
\sigma_{\text{pol}}(\mathbf{r}) &= P_{n_2}(\mathbf{r}) - P_{n_1}(\mathbf{r}) = \epsilon_0 [E_{n_2}(\mathbf{r}) - E_{n_1}(\mathbf{r})], \\
\mathbf{r} &\in S. \quad (24)
\end{aligned}$$

With the knowledge of  $\epsilon_1$  and  $\epsilon_2$  as well as the normal of the electrostatic field at one side of the interface, the polarization surface charge density can be expressed as

$$\begin{aligned}
\sigma_{\text{pol}}(\mathbf{r}) &= \epsilon_0 \left[ \frac{\epsilon_1 - \epsilon_2}{\epsilon_2} \right] E_{n_1}(\mathbf{r}) = \epsilon_0 \left[ \frac{\epsilon_1 - \epsilon_2}{\epsilon_1} \right] E_{n_2}(\mathbf{r}), \\
\mathbf{r} &\in S. \quad (25)
\end{aligned}$$

If the field increases ( $\epsilon$  reduces) as an interface is passed in the field direction,  $\sigma_{\text{pol}}$  is positive.

Given the permanent charge distributions  $\mathbf{Q} = (Q_1, Q_2, Q_3, \dots)$  and the spherical dielectric boundaries  $\mathbf{S} = (S_1, S_2, S_3, \dots)$ , where  $Q_1$  is enclosed by  $S_1$ ,  $Q_2$  by  $S_2$ , etc., the polarization surface charge densities  $\sigma_{\text{pol}} = (\sigma_{1,\text{pol}}, \sigma_{2,\text{pol}}, \sigma_{3,\text{pol}}, \dots)$  are uniquely determined. The total electrostatic energy of the system  $U$  can be expressed as

$$U = U_{\text{stat}} + U_{\text{pol}}, \quad (26)$$

where  $U_{\text{stat}}$  is the interaction energy among the permanent charge distributions and  $U_{\text{pol}}$  is the interaction energy between all permanent charge distributions and all polarization surface charge distributions.  $U_{\text{stat}}$  and  $U_{\text{pol}}$  are evaluated using relevant expressions given earlier; however, regarding  $U_{\text{pol}}$ , the expressions should be multiplied with 1/2 due to the assumption of the linear response of the media.<sup>1,2</sup>

#### V. SYSTEM OF MULTIPOLES IN SPHERICAL DIELECTRIC CAVITIES

In the following, systems comprising of electrostatic multipoles in spherical dielectric cavities immersed in a dielectric medium and some limiting cases will be considered. Throughout, our aim is to determine the polarization surface charge densities, the total electrostatic energy of the system, and the electrostatic interaction obtained by subtracting electrostatic self-energies of infinitely separated subsystems from the total electrostatic energy.

##### A. General

Consider a system consisting of  $N$  nonoverlapping subsystems in a dielectric medium, where each subsystem is composed of an electrostatic multipole localized in a spherical dielectric cavity (see Fig. 2). Subsystem  $i$ ,  $i = 1, 2, \dots, N$ , is located at  $\mathbf{R}_i = (R_i, \Omega_i)$ , possessing the spherical multipole moments,  $Q_{i,lm}$ , with respect to  $\mathbf{R}_i$  and its spherical region has the radius,  $a_i$ , and the relative dielectric permittivity,  $\epsilon_1$ . The surrounding medium has the relative dielectric permittivity  $\epsilon_2$ . The polarization surface charge density at the boundary of subsystem  $i$  is denoted by  $\sigma_i$ .

Briefly, in the following the electrostatic potential at  $\mathbf{r}_i$ ,  $r_i = a_i$  will be expressed as a superposition of terms arising from  $Q_j$  and  $\sigma_j$ ,  $j = 1, 2, \dots, N$  expanded about  $\mathbf{R}_i$ . Thereafter, the normal of the electrostatic field at  $\mathbf{r}_i$  can easily be obtained, and with Eq. (25) an equation for  $\sigma_i$  can be constructed. From the set of such  $N$  equations obtained by expansion about all  $\mathbf{R}_i$ ,  $i = 1, 2, \dots, N$ , the polarization surface charge densities  $\sigma_i$ ,  $i = 1, 2, \dots, N$ , can be solved. Finally, an expression of the interaction energy can be formulated.

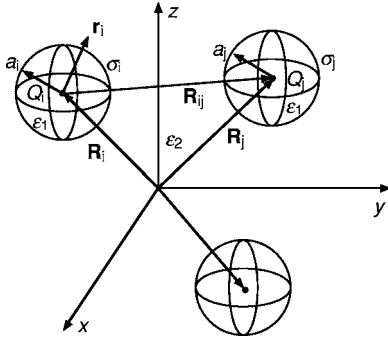


FIG. 2. Illustration of spherical multipoles, each located in a spherical dielectric cavity with relative dielectric permittivity  $\epsilon_1$ , immersed in a medium with the relative dielectric permittivity  $\epsilon_2$ . The spherical multipole,  $i$ , is characterized by its strength,  $Q_i$ , and located at  $\mathbf{R}_i$ , whereas its cavity has the radius,  $a_i$ , and the polarization surface charge densit,  $\sigma_i$ .

According to Eqs. (4) and (11), the potential at  $\mathbf{r}_i = (r_i, \Omega_i)$ ,  $r_i > a_i$  arising from  $Q_i$  and  $\sigma_i$  becomes

$$\phi_i(\mathbf{r}_i) = \frac{1}{4\pi\epsilon_0 l_{1m_1}} \left[ \frac{Q_{i,l_1 m_1}}{\epsilon_1} + a_i^{l_1} \sigma_{i,l_1 m_1} \right] \frac{1}{r_i^{l_1+1}} C_{l_1 m_1}^*(\Omega_i), \quad (27)$$

where  $\sigma_{i,l_1 m_1}$  is given by Eq. (9). The potential at  $\mathbf{R}_j + \mathbf{r}_j$ ,  $\mathbf{r}_j = (r_j, \Omega_j)$ ,  $r_j > a_j$ , generated by  $Q_j$  and by  $\sigma_j$ ,  $j \neq i$ , expanded about  $\mathbf{R}_j$  is given analogously. Now, we need to translate the expansion center of  $Q_j$  and  $\sigma_j$  from  $\mathbf{R}_j$  to  $\mathbf{R}_i$ . By the use of Eq. (21), the potential generated by  $Q_j$  and  $\sigma_j$  at  $\mathbf{r}_i$ ,  $r_i < R_{ij} - a_j$ , can be expressed as

$$\begin{aligned} \phi_j(\mathbf{r}_i) &= \frac{1}{4\pi\epsilon_0 l_{1m_1}} \sum_{l_2 m_2} (-1)^{l_1+M} f(l_1, l_2, m_1, m_2) \\ &\times \left[ \frac{Q_{j,l_2 m_2}}{\epsilon_1} + a_j^{l_2} \sigma_{j,l_2 m_2} \right] r_i^{l_1} C_{l_1 m_1}(\Omega_i) \\ &\times \frac{1}{R_{ij}^{L+1}} C_{LM}^*(\Omega_{ij}), \end{aligned} \quad (28)$$

where we here for convenience have introduced

$$\begin{aligned} f(l_1, l_2, m_1, m_2) &= \left[ \frac{(2L)!}{(2l_1)! (2l_2)!} \right]^{1/2} \sqrt{2L+1} \begin{pmatrix} l_1 & l_2 & L \\ m_1 & m_2 & -M \end{pmatrix}, \end{aligned} \quad (29)$$

and  $L \equiv l_1 + l_2$  and  $M \equiv m_1 + m_2$ . The total potential at  $\mathbf{r}_i$ ,  $a_i < r_i < R_{ij} - a_j$ , arising from  $N$  subsystems is obtained through

$$\phi(\mathbf{r}_i) = \phi_i(\mathbf{r}_i) + \sum_{j \neq i} \phi_j(\mathbf{r}_i). \quad (30)$$

Now, (i) substitution of Eqs. (27) and (28) into Eq. (30), (ii) obtaining the field normal to the dielectric discontinuity  $E_{n,2}(r_i)$  according to Eq. (13), (iii) insertion of  $E_{n,2}(r_i)$  into Eq. (25) to obtain the surface charge density  $\sigma_i$ , and (iv) insertion of  $\sigma_i$  in Eq. (9) and solving for the spherical surface

charge multipole moments  $\sigma_{i,l_1 m_1}$ ,  $i=1, 2, \dots, N$ , results in

$$\begin{aligned} \sigma_{i,l_1 m_1} &= -\frac{\epsilon_2 - \epsilon_1}{\epsilon_2 + \frac{l_1}{l_1+1} \epsilon_1} \left\{ \frac{Q_{i,l_1 m_1}}{\epsilon_1} \frac{1}{a_i^{l_1}} - \frac{l_1}{l_1+1} a_i^{l_1+1} \right. \\ &\times \sum_{l_2 m_2} (-1)^{l_1+M} f(l_1, l_2, m_1, m_2) \\ &\times \sum_{j \neq i} \left[ \frac{Q_{j,l_2 m_2}^*}{\epsilon_1} + a_j^{l_2} \sigma_{j,l_2 m_2}^* \right] \left. \frac{1}{R_{ij}^{L+1}} C_{LM}(\Omega_{ij}) \right\}. \end{aligned} \quad (31)$$

We notice that  $\sigma_{i,00}$ ,  $i=1, 2, \dots, N$  are decoupled from the remaining multipole moments and are independent on the positions of the subsystems.

According to Eq. (26) and the following discussion, the total electrostatic energy of the system can be expressed as

$$U = U_{\text{stat}} + U_{\text{pol}},$$

$$U_{\text{stat}} = \sum_i \sum_{j>i} U_{Q_i Q_j},$$

$$U_{\text{pol}} = \frac{1}{2} \left[ \sum_i \sum_{j \neq i} U_{\sigma_i Q_j} + \sum_i U_{\sigma_i \sigma_i} \right], \quad (32)$$

where  $U_{Q_i Q_j}$  denotes the electrostatic interaction between the electrostatic multipoles  $Q_i$  and  $Q_j$ ;  $U_{\sigma_i Q_j}$  denotes the electrostatic interaction between the polarization surface charge density  $\sigma_i$  and the electrostatic multipole  $Q_j$ ,  $j \neq i$ ; and  $U_{\sigma_i \sigma_i}$  denotes the electrostatic interaction between the polarization surface charge density  $\sigma_i$  and the electrostatic multipole  $Q_i$ . With the use of Eqs. (19), (10), and (16), the following expressions for  $U_{Q_i Q_j}$ ,  $U_{\sigma_i Q_j}$ , and  $U_{\sigma_i \sigma_i}$  are obtained:

$$\begin{aligned} U_{Q_i Q_j} &= \frac{1}{4\pi\epsilon_0 \epsilon_1} \\ &\times \sum_{l_1 m_1} \sum_{l_2 m_2} (-1)^{l_1+M} f(l_1, l_2, m_1, m_2) Q_{i,l_1 m_1} Q_{j,l_2 m_2} \\ &\times \frac{1}{R_{ij}^{L+1}} C_{LM}^*(\Omega_{ij}), \end{aligned}$$

$$\begin{aligned} U_{\sigma_i Q_j} &= \frac{1}{4\pi\epsilon_0} \\ &\times \sum_{l_1 m_1} \sum_{l_2 m_2} (-1)^{l_1+M} f(l_1, l_2, m_1, m_2) a_i^{l_1} \sigma_{i,l_1 m_1} Q_{j,l_2 m_2} \\ &\times \frac{1}{R_{ij}^{L+1}} C_{LM}^*(\Omega_{ij}), \end{aligned}$$

$$U_{\sigma_i \sigma_i} = \frac{1}{4\pi\epsilon_0} \sum_{lm} \frac{1}{a_i^{l+1}} \sigma_{i,lm}^* \sigma_{i,lm}. \quad (33)$$

The interaction energy of the system with respect to mutual infinite separation among the subsystems ( $R_{ij} \equiv |\mathbf{R}_j - \mathbf{R}_i| \rightarrow \infty, \forall ij$ ) becomes

$$U_{\text{int}} \equiv U - U(R_{ij} \rightarrow \infty, \forall ij), \quad (34)$$

where  $U$  is given by Eqs. (32) and (33) and  $U(R_{ij} \rightarrow \infty, \forall ij)$  is given by

$$U(R_{ij} \rightarrow \infty, \forall ij) = -\frac{1}{4\pi\epsilon_0\epsilon_1} \frac{1}{2} \sum_i \sum_{lm} \frac{\epsilon_2 - \epsilon_1}{\epsilon_2 + \frac{l}{l+1}\epsilon_1} \frac{1}{a_i^{2l+1}} |Q_{i,lm}|^2. \quad (35)$$

Equation (31) specifying the spherical surface charge multipole moments,  $\sigma_{i,lm}$ ,  $i=1,2,\dots,N$ , and Eqs. (32)–(35) specifying the total electrostatic energy,  $U$ , and interaction energy,  $U_{\text{int}}$ , of the system constitute the main results of the present work. In the following, corresponding expressions for simplified systems will be given.

## B. System of monopoles in cavities

We will simplify by assuming that multipole  $i$  is a point charge in the center of sphere  $i$ , hence,  $Q_{i,lm} = q_i \delta_{l0} \delta_{m0}$ ,  $i=1,2,\dots,N$ . With these monopoles, we get from Eq. (31) after some simplifications

$$\sigma_{i,00} = -\frac{\epsilon_2 - \epsilon_1}{\epsilon_2} \frac{q_i}{\epsilon_1} \quad (36)$$

and

$$\begin{aligned} \sigma_{i,l_1 m_1} = & -\frac{\epsilon_2 - \epsilon_1}{\epsilon_2 + \frac{l_1}{l_1+1}\epsilon_1} \\ & \times \left\{ -\frac{l_1}{l_1+1} a_i^{l_1+1} \left[ \sum_{j \neq i} \frac{q_j}{\epsilon_2 R_{ij}^{l_1+1}} C_{l_1 m_1}(\Omega_{ij}) \right. \right. \\ & + \sum_{l_2 \geq 1, m_2} (-1)^{l_1+m_2} f(l_1, l_2, m_1, m_2) \sum_{j \neq i} a_j^{l_2} \sigma_{j, l_2 m_2}^* \\ & \left. \left. \times \frac{1}{R_{ij}^{l_1+1}} C_{LM}(\Omega_{ij}) \right] \right\}, \end{aligned}$$

$$l_1 \geq 1, \quad (37)$$

where the terms involving the factors  $q_j/\epsilon_1$  and  $\sigma_{j,00}$  have been merged to give the term with the factor  $q_j/\epsilon_2$ , and hence, the summation over  $l_2$  starts from 1. After some manipulation, the electrostatic energy contributions become

$$\begin{aligned} U_{q_i q_j} &= \frac{1}{4\pi\epsilon_0\epsilon_1} \frac{q_i q_j}{R_{ij}}, \\ U_{\sigma_i q_j} &= \frac{1}{4\pi\epsilon_0} \left[ -\frac{\epsilon_2 - \epsilon_1}{\epsilon_1 \epsilon_2} \frac{q_i q_j}{R_{ij}} + q_j \sum_{l \geq 1, m} \frac{a_i^l \sigma_{i,lm}}{R_{ij}^{l+1}} C_{lm}^*(\Omega_{ij}) \right], \\ U_{\sigma_i \sigma_j} &= -\frac{1}{4\pi\epsilon_0\epsilon_1} \frac{\epsilon_2 - \epsilon_1}{\epsilon_2} \frac{q_i^2}{a_i}, \end{aligned} \quad (38)$$

and the interaction energy as defined by Eq. (34) becomes

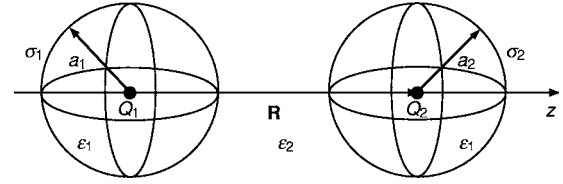


FIG. 3. Illustration of the two spherical multipoles,  $Q_1$  and  $Q_2$ , each located in the center of a dielectric sphere with the relative dielectric permittivity,  $\epsilon_1$ , radii,  $a_1$  and  $a_2$ , and the polarization surface charges,  $\sigma_1$  and  $\sigma_2$ , respectively, immersed in a medium with the relative dielectric permittivity,  $\epsilon_2$ .

$$U_{\text{int}} = \sum_i \sum_{j>i} \tilde{U}_{q_i q_j} + \frac{1}{2} \sum_i \sum_{j \neq i} \tilde{U}_{\sigma_i \sigma_j},$$

$$\tilde{U}_{q_i q_j} = \frac{1}{4\pi\epsilon_0\epsilon_2} \frac{q_i q_j}{R_{ij}},$$

$$\tilde{U}_{\sigma_i \sigma_j} = \frac{1}{4\pi\epsilon_0} q_j \sum_{l \geq 1, m} \frac{a_i^l \sigma_{i,lm}}{R_{ij}^{l+1}} C_{lm}^*(\Omega_{ij}). \quad (39)$$

Here half of the sum of the first terms of  $U_{\sigma_i q_j}$  and  $U_{\sigma_j q_i}$  in Eq. (38) have been merged with  $U_{q_i q_j}$  to form  $\tilde{U}_{q_i q_j}$ , leading to an apparent change of the dielectric screening from  $1/\epsilon_1$  to  $1/\epsilon_2$  of the interaction among the monopoles. In the limit of vanishing spherical cavities,  $\tilde{U}_{\sigma_i \sigma_j}$ ,  $\forall ij$ , is zero, and the interaction energy provides the picture that Coulomb law is operating, but the electrostatic interaction being attenuated with the relative dielectric permittivity of the medium.

## C. Two multipoles

We will now continue with the special case of a system composed of two subsystems, labeled 1 and 2 (see Fig. 3). Moreover, without loss of generality,  $\mathbf{R}_{12}$  is parallel to the  $z$  axis leading to  $C_{LM}(\Omega_{12}) = \delta_{M0}$  and  $-m_2 = m_1$ . For simplicity, we introduce  $\mathbf{R} = \mathbf{R}_{12}$  and  $m = -m_2 = m_1$ . From Eq. (31) and with help of Eq. (6) we obtain

$$\begin{aligned} \sigma_{1, l_1 m} = & -\frac{\epsilon_2 - \epsilon_1}{\epsilon_2 + \frac{l_1}{l_1+1}\epsilon_1} \left\{ \frac{Q_{1, l_1 m}}{\epsilon_1} \frac{1}{a_1^{l_1}} - \frac{l_1}{l_1+1} a_1^{l_1+1} \right. \\ & \times \sum_{l_2} (-1)^{l_1+m} f(l_1, l_2, m, -m) \\ & \left. \times \left[ \frac{Q_{2, l_2 m}}{\epsilon_1} + a_2^{l_2} \sigma_{2, l_2 m} \right] \frac{1}{R^{l_1+1}} \right\}. \end{aligned} \quad (40)$$

A few comments: (i) By symmetry,  $\sigma_{2, l_1 m}$  is obtained by swapping system indices 1 and 2 and multiplication of the  $1/R^{l_1+1}$  terms by the phase factor  $(-1)^{l_1}$ . (ii) As before, the components  $\sigma_{1,00}$  and  $\sigma_{2,00}$  are decoupled from the remaining ones. (iii) For a fully axial symmetry, only terms in Eq. (40) with  $m=0$  contribute and the  $f$  function reduces to  $f(l_1, l_2, 0, 0) = (-1)^{l_1+l_2} (l_1+l_2)! / (l_1! l_2!)$ .

The total electrostatic energy of the system becomes

$$\begin{aligned}
U &= U_{\text{stat}} + U_{\text{pol}}, \\
U_{\text{stat}} &= U_{Q_1 Q_2}, \\
U_{\text{pol}} &= \frac{1}{2}[(U_{\sigma_1 Q_2} + U_{\sigma_2 Q_1}) + (U_{\sigma_1 Q_1} + U_{\sigma_2 Q_2})], \quad (41)
\end{aligned}$$

with

$$\begin{aligned}
U_{Q_1 Q_2} &= \frac{1}{4\pi\epsilon_0\epsilon_1} \sum_{l_1} \sum_{l_2} \sum_m (-1)^{l_1} f(l_1, l_2, m, -m) \\
&\quad \times Q_{1, l_1 m} Q_{2, l_2 - m} \frac{1}{R^{L+1}}, \\
U_{\sigma_1 Q_2} &= \frac{1}{4\pi\epsilon_0} \sum_{l_1} \sum_{l_2} \sum_m (-1)^{l_1} f(l_1, l_2, m, -m) \\
&\quad \times a_1^{l_1} \sigma_{1, l_1 m} Q_{2, l_2 - m} \frac{1}{R^{L+1}}, \\
U_{\sigma_1 Q_1} &= \frac{1}{4\pi\epsilon_0} \sum_{lm} \frac{1}{a_1^{l+1}} \sigma_{1, lm}^* Q_{1, lm}, \quad (42)
\end{aligned}$$

and  $U_{\sigma_2 Q_1}$  and  $U_{\sigma_2 Q_2}$  obtained by swapping system indices 1 and 2 and multiplication of the  $1/R^{L+1}$  terms by the phase factor  $(-1)^L$  in the expressions of  $U_{\sigma_1 Q_2}$  and  $U_{\sigma_1 Q_1}$ , respectively. The interaction energy is still given by Eqs. (34) and (35), but the summation over subsystems in Eq. (35) is restricted to subsystems 1 and 2.

#### D. Two monopoles

We will again consider a system composed of two subsystems, but now they possess only monopoles, i.e.,  $Q_{1, l_1 m_1} = q_1 \delta_{l_1 0} \delta_{m_1 0}$  and  $Q_{2, l_2 m_2} = q_2 \delta_{l_2 0} \delta_{m_2 0}$ . Again we let  $\mathbf{R}$  be parallel to the  $z$  axis. With these monopoles, we get from Eq. (40),

$$\begin{aligned}
\sigma_{1,00} &= -\frac{\epsilon_2 - \epsilon_1 q_1}{\epsilon_2 \epsilon_1}, \quad (43) \\
\sigma_{1, l_1 m} &= -\frac{\epsilon_2 - \epsilon_1}{\epsilon_2 + \frac{l_1}{l_1+1} \epsilon_1} \left\{ -\frac{l_1}{l_1+1} a_1^{l_1+1} \left[ \frac{q_2 \delta_{m0}}{\epsilon_2} \frac{1}{R^{l_1+1}} \right. \right. \\
&\quad \left. \left. + \sum_{l_2 \geq 1} (-1)^{l_1+m} f(l_1, l_2, m, -m) \sigma_{2, l_2 m} \frac{1}{R^{L+1}} \right] \right\}, \\
l_1 &\geq 1, \quad (44)
\end{aligned}$$

and similar expressions for  $\sigma_{2, lm}$ . Furthermore, the insertion of Eqs. (43) and (44) into Eq. (42) results in the electrostatic energy contributions

$$\begin{aligned}
U_{q_1 q_2} &= \frac{1}{4\pi\epsilon_0\epsilon_1} \frac{q_1 q_2}{R}, \\
U_{\sigma_1 q_2} &= \frac{1}{4\pi\epsilon_0} \left[ -\frac{\epsilon_2 - \epsilon_1 q_1 q_2}{\epsilon_1 \epsilon_2} \frac{1}{R} + q_2 \sum_{l \geq 1} \frac{a_1^l \sigma_{1, l 0}}{R^{l+1}} \right],
\end{aligned}$$

$$U_{\sigma_1 q_1} = -\frac{1}{4\pi\epsilon_0\epsilon_1} \frac{\epsilon_2 - \epsilon_1 q_1^2}{\epsilon_2 a_1}, \quad (45)$$

whereas the interaction energy with respect to two infinitely separated subsystems  $U_{\text{int}}$  becomes

$$\begin{aligned}
U_{\text{int}} &= \tilde{U}_{q_1 q_2} + \frac{1}{2}(\tilde{U}_{\sigma_1 q_2} + \tilde{U}_{\sigma_2 q_1}), \\
\tilde{U}_{q_1 q_2} &= \frac{1}{4\pi\epsilon_0\epsilon_2} \frac{q_1 q_2}{R}, \\
\tilde{U}_{\sigma_1 q_2} &= \frac{1}{4\pi\epsilon_0} q_2 \sum_{l \geq 1} \frac{a_1^l \sigma_{1, l 0}}{R^{l+1}}. \quad (46)
\end{aligned}$$

We will now consider two special cases. The first one comprises a truncation of the expansion of  $\sigma_1$  and  $\sigma_2$  and solving the surface charge multipole moments analytically. With the truncation of the expansion of  $\sigma_1$  and  $\sigma_2$  to  $l \leq 1$ , Eq. (40) gives

$$\begin{aligned}
\sigma_{1,00} &= -\frac{\epsilon_2 - \epsilon_1 q_1}{\epsilon_2 \epsilon_1}, \\
\sigma_{1,10} &= \frac{\epsilon_2 - \epsilon_1}{\epsilon_2 + \frac{1}{2}\epsilon_1} \left[ \frac{a_1^2 q_2}{2R^2 \epsilon_1} + \frac{a_1^2}{2R^2} \sigma_{2,00} - \frac{a_1^2 a_2}{R^3} \sigma_{2,10} \right], \\
\sigma_{1,1\pm 1} &= -\frac{\epsilon_2 - \epsilon_1}{\epsilon_2 + \frac{1}{2}\epsilon_1} \frac{a_1^2 a_2}{2R^3} \sigma_{2,1\pm 1}, \quad (47)
\end{aligned}$$

and a similar set of equations for  $\sigma_{2, lm}$ . The solution of these two sets of linear equations becomes

$$\begin{aligned}
\sigma_{1,00} &= -\frac{\epsilon_2 - \epsilon_1 q_1}{\epsilon_2 \epsilon_1}, \\
\sigma_{2,00} &= -\frac{\epsilon_2 - \epsilon_1 q_2}{\epsilon_2 \epsilon_1}, \quad (48) \\
\sigma_{1,10} &= \frac{1}{2} \left( \frac{\epsilon_2 - \epsilon_1}{\epsilon_2 + \frac{1}{2}\epsilon_1} \right) \frac{a_1^2 q_2}{R^2 \epsilon_2} + \frac{1}{2} \left( \frac{\epsilon_2 - \epsilon_1}{\epsilon_2 + \frac{1}{2}\epsilon_1} \right)^2 \frac{a_1^2 a_2^3 q_1}{R^5 \epsilon_2} \\
&\quad + O(R^{-8}), \\
\sigma_{2,10} &= -\frac{1}{2} \left( \frac{\epsilon_2 - \epsilon_1}{\epsilon_2 + \frac{1}{2}\epsilon_1} \right) \frac{a_2^2 q_1}{R^2 \epsilon_2} - \frac{1}{2} \left( \frac{\epsilon_2 - \epsilon_1}{\epsilon_2 + \frac{1}{2}\epsilon_1} \right)^2 \frac{a_2^2 a_1^3 q_2}{R^5 \epsilon_2} \\
&\quad + O(R^{-8}), \quad (49)
\end{aligned}$$

$$\begin{aligned}
\sigma_{1,1\pm 1} &= 0, \\
\sigma_{2,1\pm 1} &= 0. \quad (50)
\end{aligned}$$

The insertion of the spherical surface charge multipole moments given by Eq. (49) into Eq. (45) gives

$$U_{q_1 q_2} = \frac{1}{4\pi\epsilon_0\epsilon_1} \frac{q_1 q_2}{R},$$



$$U_{\sigma_1 q_2} = \frac{1}{4\pi\epsilon_0} \left[ -\frac{\epsilon_2 - \epsilon_1}{\epsilon_1 \epsilon_2} \frac{q_1 q_2}{R} + \frac{1}{2} \left( \frac{\epsilon_2 - \epsilon_1}{\epsilon_2 + \frac{1}{2}\epsilon_1} \right) \frac{a_1^3 q_2^2}{R^4 \epsilon_2} \right. \\ \left. + \frac{1}{2} \left( \frac{\epsilon_2 - \epsilon_1}{\epsilon_2 + \frac{1}{2}\epsilon_1} \right)^2 \frac{a_1^3 a_2^3 q_1 q_2}{R^7 \epsilon_2} + O(R^{-8}) \right], \\ U_{q_1 \sigma_1} = -\frac{1}{4\pi\epsilon_0 \epsilon_1} \frac{\epsilon_2 - \epsilon_1}{\epsilon_2} \frac{q_1^2}{a_1}, \quad (51)$$

and with the analogous expressions for  $U_{\sigma_2 q_1}$  and  $U_{\sigma_2 q_2}$  we have

$$U = \frac{1}{4\pi\epsilon_0} \left[ -\frac{1}{2} \frac{\epsilon_2 - \epsilon_1}{\epsilon_1 \epsilon_2} \left( \frac{q_1^2}{a_1} + \frac{q_2^2}{a_2} \right) + \frac{1}{\epsilon_1} \frac{q_1 q_2}{R} \right. \\ \left. - \frac{\epsilon_2 - \epsilon_1}{\epsilon_1 \epsilon_2} \frac{q_1 q_2}{R} + \frac{1}{4} \left( \frac{\epsilon_2 - \epsilon_1}{\epsilon_2 + \frac{1}{2}\epsilon_1} \right) \frac{1}{\epsilon_2} \frac{a_2^3 q_1^2 + a_1^3 q_2^2}{R^4} \right. \\ \left. + O(R^{-6}) \right]. \quad (52)$$

The  $O(R^{-7})$  has been dropped since other energy terms of the order  $O(R^{-6})$  are missing owing from the truncation in  $l$ . Eventually, the interaction energy of the two subsystems becomes

$$U_{\text{int}} \equiv U - U(R \rightarrow \infty) = \frac{1}{4\pi\epsilon_0 \epsilon_2} \left[ \frac{q_1 q_2}{R} \right. \\ \left. + \frac{1}{4} \left( \frac{\epsilon_2 - \epsilon_1}{\epsilon_2 + \frac{1}{2}\epsilon_1} \right) \frac{a_2^3 q_1^2 + a_1^3 q_2^2}{R^4} + O(R^{-6}) \right], \quad (53)$$

where the first term represents the electrostatic interaction of the two charges screened by their polarization monopoles, and the second term represents the repulsion between the screened charge and the polarization dipole at the other subsystem. Hence, we have provided a physical interpretation of the leading terms of the interaction between two point charges each located in a spherical dielectric cavity. A more extensive model, but in the limit of no induced dipole moments and only point charges, reducing to Eq. (53) with  $\epsilon_1 = 1$  has been presented,<sup>30</sup> and the second term of Eq. (53) originating from the presence of cavities has been included in effective ion-ion potentials for aqueous 1-1 electrolytes but found to be small in magnitude.<sup>31</sup>

The second case comprises the limit  $a_2 \rightarrow 0$ , i.e., when the dielectric cavity of subsystem 2 is negligible. The insertion of  $a_2 = 0$  in Eq. (44) gives  $\sigma_{2,lm} = 0$ ,  $l \geq 1$ . This, together with Eqs. (43) and (44), results in

$$\sigma_{1,00} = -\frac{\epsilon_2 - \epsilon_1}{\epsilon_2} \frac{q_1}{\epsilon_1}, \\ \sigma_{1,lm} = \frac{l}{l+1} \frac{\epsilon_2 - \epsilon_1}{\epsilon_2 + \frac{1}{l+1}\epsilon_1} \frac{a_1^{l+1}}{R^{l+1}} \frac{q_2}{\epsilon_2} \delta_{m0}, \quad l \geq 1, \\ \sigma_{2,lm} = -\frac{\epsilon_2 - \epsilon_1}{\epsilon_2} \frac{q_2}{\epsilon_1} \delta_{l0} \delta_{m0}. \quad (54)$$

Furthermore, the insertion of the surface charge multipole moments into Eq. (46) gives the interaction energy

$$U_{\text{int}} = \frac{1}{4\pi\epsilon_0 \epsilon_2} \left[ \frac{q_1 q_2}{R} + \frac{1}{2} \sum_{l \geq 1} \frac{l}{l+1} \frac{\epsilon_2 - \epsilon_1}{\epsilon_2 + \frac{1}{l+1}\epsilon_1} \frac{a_1^{2l+1}}{R^{2l+2}} q_2^2 \right]. \quad (55)$$

There is here a subtlety. A direct assumption  $a_2 = 0$  before solving the dielectric boundary conditions leads to an inconsistency. The dielectric screening of the electrostatic interaction between monopoles  $q_1$  and  $q_2$  becomes ill-defined, since  $q_1$  would then reside in a medium with the relative dielectric permittivity  $\epsilon_1$  and  $q_2$  in a medium with the relative dielectric permittivity  $\epsilon_2 \neq \epsilon_1$ .

Finally, the total electrostatic potential at  $r > a_1$  is given according to

$$\phi(\mathbf{r}) = \phi_{q_1}(\mathbf{r}) + \phi_{q_2}(\mathbf{r}) + \phi_{\sigma_1}(\mathbf{r}) \\ = \frac{1}{4\pi\epsilon_0 \epsilon_2} \left[ \frac{1}{r} q_1 + \left( \frac{1}{|\mathbf{r} - \mathbf{R}|} \right. \right. \\ \left. \left. + \sum_l \frac{l}{l+1} \frac{\epsilon_2 - \epsilon_1}{\epsilon_2 + \frac{1}{l+1}\epsilon_1} \frac{a_1^{2l+1}}{R^{l+1}} \frac{1}{r^{l+1}} P_l(\cos \gamma) \right) q_2 \right], \quad (56)$$

where Eq. (11) has been used and the  $\gamma$  denotes the angle between  $\mathbf{r}$  and the  $z$  axis. The reaction field at  $r > a_1$  arising from the polarization surface charge density becomes

$$\phi_{\sigma_1}(\mathbf{r}) = \frac{1}{4\pi\epsilon_0} \left[ -\frac{\epsilon_2 - \epsilon_1}{\epsilon_2} \frac{1}{r} \frac{q_1}{\epsilon_2} \right. \\ \left. + \left( \sum_l \frac{l}{l+1} \frac{\epsilon_2 - \epsilon_1}{\epsilon_2 + \frac{1}{l+1}\epsilon_1} \frac{a_1^{2l+1}}{R^{l+1}} \frac{1}{r^{l+1}} P_l(\cos \gamma) \right) \frac{q_2}{\epsilon_2} \right], \quad (57)$$

an expression (in particular after the omission of the first term that is due to charge  $q_1$ ) that has frequently appeared in the literature.<sup>1,14-16</sup>

## E. Two dipoles

Instead of only monopoles, we will now make the restriction that we have only dipoles, i.e.,  $Q_{1,l_1 m_1} \neq 0$  only for  $l_1 = 1$  and  $Q_{2,l_2 m_2} \neq 0$  only for  $l_2 = 1$ . The relation between the Cartesian and standard forms of the dipole moments is

$$Q_{10} = p_z, \\ Q_{11} = -\frac{1}{\sqrt{2}}(p_x + ip_y), \\ Q_{1-1} = \frac{1}{\sqrt{2}}(p_x - ip_y), \\ p_x = -\frac{1}{\sqrt{2}}(Q_{11} - Q_{1-1}), \\ p_y = \frac{i}{\sqrt{2}}(Q_{11} + Q_{1-1}), \\ p_z = Q_{10}. \quad (58)$$

Again we let  $\mathbf{R}$  be parallel to the  $z$  axis. With these dipoles, we get from Eq. (40),

$$\sigma_{1,00} = 0, \quad (59)$$

$$\sigma_{1,l_1 m} = -\frac{\varepsilon_2 - \varepsilon_1}{\varepsilon_2 + \frac{l_1}{l_1+1}\varepsilon_1} \left\{ \frac{Q_{1,l_1 m} \delta_{l_1 1}}{\varepsilon_1} \frac{1}{a_1^{l_1}} - \frac{l_1}{l_1+1} a_1^{l_1+1} \right. \\ \times \left[ (-1)^{l_1+m} f(l_1, 1, m, -m) \frac{Q_{2,l_1 m}}{\varepsilon_1} \frac{1}{R^{l_1+2}} \right. \\ \left. \left. + \sum_{l_2} (-1)^{l_1+m} f(l_1, l_2, m, -m) a_2^{l_2} \sigma_{2,l_2 m} \frac{1}{R^{l_1+1}} \right] \right\}, \\ l_1 \geq 1, \quad (60)$$

and from Eq. (33) we get the electrostatic energy contributions

$$U_{p_1 p_2} = \frac{1}{4\pi\varepsilon_0\varepsilon_1} \sum_m (-1)^m f(1, 1, m, -m) Q_{1,1m} Q_{2,1-m} \frac{1}{R^3}, \\ U_{\sigma_1 p_2} = \frac{1}{4\pi\varepsilon_0} \sum_{l_1} \sum_m (-1)^{l_1+m} \\ \times f(l_1, 1, m, -m) a_1^{l_1} \sigma_{1,l_1 m} Q_{2,1-m} \frac{1}{R^{l_1+2}}, \\ U_{\sigma_1 p_1} = \frac{1}{4\pi\varepsilon_0} \sum_m \frac{1}{a_1^2} \sigma_{1,1m}^* Q_{1,1m}. \quad (61)$$

Also here we will consider a truncation of the expansion of  $\sigma_1$  and  $\sigma_2$  and solve the surface charge multipole moments analytically. With the truncation of the expansion of  $\sigma_1$  and  $\sigma_2$  to  $l \leq 1$ , Eqs. (59) and (60) give

$$\sigma_{1,00} = 0, \\ \sigma_{1,10} = -\alpha \left[ \frac{1}{a_1} \frac{Q_{1,10}}{\varepsilon_1} - \frac{1}{2} \frac{a_1^2}{R^2} \sigma_{2,00} + \frac{a_1^2}{R^3} \frac{Q_{2,10}}{\varepsilon_1} \right. \\ \left. + \frac{a_1^2 a_2}{R^3} \sigma_{2,10} \right], \\ \sigma_{1,1\pm 1} = -\alpha \left[ \frac{1}{a_1} \frac{Q_{1,1\pm 1}}{\varepsilon_1} - \frac{1}{2} \frac{a_1^2}{R^3} \frac{Q_{2,1\pm 1}}{\varepsilon_1} - \frac{1}{2} \frac{a_1^2 a_2}{R^3} \sigma_{2,1\pm 1} \right], \quad (62)$$

and a similar set of equations for  $\sigma_{2,lm}$ . The solution of these two sets of linear equations becomes

$$\sigma_{1,00} = 0, \\ \sigma_{2,00} = 0, \\ \sigma_{1,10} = -\alpha \frac{1}{a_1} \frac{Q_{1,10}}{\varepsilon_1} - \alpha(1-\alpha) \frac{a_1^2}{R^3} \frac{Q_{2,10}}{\varepsilon_1} \\ + \alpha^2(1-\alpha) \frac{a_1^2 a_2^3}{R^6} \frac{Q_{1,10}}{\varepsilon_1} + O(R^{-9}),$$

$$\sigma_{2,10} = -\alpha \frac{1}{a_2} \frac{Q_{2,10}}{\varepsilon_1} - \alpha(1-\alpha) \frac{a_2^2}{R^3} \frac{Q_{1,10}}{\varepsilon_1} \\ + \alpha^2(1-\alpha) \frac{a_2^2 a_1^3}{R^6} \frac{Q_{2,10}}{\varepsilon_1} + O(R^{-9}), \quad (64)$$

$$\sigma_{1,11} = -\alpha \frac{1}{a_1} \frac{Q_{1,11}}{\varepsilon_1} + \frac{1}{2} \alpha(1-\alpha) \frac{a_1^2}{R^3} \frac{Q_{2,11}}{\varepsilon_1} \\ + \frac{1}{4} \alpha^2(1-\alpha) \frac{a_1^2 a_2^3}{R^6} \frac{Q_{1,11}}{\varepsilon_1} + O(R^{-9}),$$

$$\sigma_{2,11} = -\alpha \frac{1}{a_2} \frac{Q_{2,11}}{\varepsilon_1} + \frac{1}{2} \alpha(1-\alpha) \frac{a_2^2}{R^3} \frac{Q_{1,11}}{\varepsilon_1} \\ + \frac{1}{4} \alpha^2(1-\alpha) \frac{a_2^2 a_1^3}{R^6} \frac{Q_{2,11}}{\varepsilon_1} + O(R^{-9}). \quad (65)$$

The insertion of Eqs. (63)–(65) into Eq. (61) and the analogous expressions for  $U_{\sigma_2 p_1}$  and  $U_{\sigma_2 p_2}$  give eventually the interaction energy after using Eq. (58),

$$U_{\text{int}} \equiv U - U(R \rightarrow \infty) \\ = -\frac{1}{4\pi\varepsilon_0\varepsilon_2} \left( \frac{3\varepsilon_2}{2\varepsilon_2 + \varepsilon_1} \right)^2 \frac{3(\mathbf{p}_1 \cdot \hat{\mathbf{z}})(\mathbf{p}_2 \cdot \hat{\mathbf{z}}) - (\mathbf{p}_1 \cdot \mathbf{p}_2)}{R^3} \\ + O(R^{-6}). \quad (66)$$

Thus, a dipole in a spherical cavity with the relative dielectric permittivity  $\varepsilon_1$  (and even in the limit of a zero radius) in a dielectric medium with the relative dielectric permittivity  $\varepsilon_2$  appears to have a dipole moment larger than the microscopic one, where the limiting enhancement factor 3/2 is achieved when  $\varepsilon_2 \gg \varepsilon_1$ . This appearance was first established by considering the electrostatic field in the dielectric emanating from one dipole in a cavity,<sup>24,25</sup> and later derived for two dipoles, each in one cavity.<sup>20</sup>

## VI. NUMERICAL EXAMPLES

Some selected examples illustrating the effect of the surface polarization at dielectric discontinuities on the interaction energy will now be provided. We will consider systems possessing either two or three subsystems, where each subsystem is composed of a charge or a dipole localized at the center of a spherical region with the relative dielectric permittivity  $\varepsilon_1$ , immersed in a medium characterized by  $\varepsilon_2$ . For simplicity, we assume equal absolute charge  $q_i = |q|$ , equal magnitude of the dipole moments  $p_i = p$ , and equal radius  $a_i = a$ . Each system will be examined at two different dielectric conditions: spheres with  $\varepsilon_1 = 1$  in a medium with  $\varepsilon_2 = 80$  (case A) and spheres with  $\varepsilon_1 = 80$  in a medium with  $\varepsilon_2 = 1$  (case B). Case A could correspond to low-dielectric particles carrying a charge or dipole moment in water, whereas case B to charged water droplets in oil or air.

The effect of the surface polarization will be examined by considering the reduced interaction energy  $U_{\text{int}}^{\text{red}}$  defined according to

$$U_{\text{int}}^{\text{red}} \equiv \frac{U_{\text{int}}}{\lim_{a_i \rightarrow 0, \forall i} U_{\text{int}}}, \quad (67)$$

where the interaction energy  $U_{\text{int}}$  is given by Eq. (34). In the case of charges the denominator simplifies to

$$\lim_{a_i \rightarrow 0, \forall i} U_{\text{int}} = \sum_i \sum_{j>i} \frac{1}{4\pi\epsilon_0\epsilon_2} \frac{q_i q_j}{R_{ij}}, \quad (68)$$

and in the case of dipoles to

$$\lim_{a_i \rightarrow 0, \forall i} U_{\text{int}} = \sum_i \sum_{j>i} (-1) \frac{1}{4\pi\epsilon_0\epsilon_2} \left( \frac{3\epsilon_2}{2\epsilon_2 + \epsilon_1} \right)^2 \times \frac{3(\mathbf{p}_i \cdot \mathbf{R}_{ij})(\mathbf{p}_j \cdot \mathbf{R}_{ij}) - (\mathbf{p}_i \cdot \mathbf{p}_j)}{R_{ij}^3}. \quad (69)$$

Hence,  $U_{\text{int}}^{\text{red}}$  represents the ratio of the interaction energy with the cavities present and the interaction energy for the corresponding system but with zero cavity radii, i.e., the charges or the dipoles appear in a homogeneous medium characterized by the relative dielectric permittivity  $\epsilon_2$ . Note, in the case of dipoles the  $[3\epsilon_2/(2\epsilon_2 + \epsilon_1)]^2$  factor appears, resulting in the limit  $U_{\text{int}}^{\text{red}} \rightarrow 1$  for infinitely separated dipoles. In the following, we will monitor  $U_{\text{int}}^{\text{red}}$  as a function of  $R/2a$ , a single parameter used to characterize the relative positions of the subsystems, with  $R/(2a)=1$  being the lower limit corresponding to sphere contact. Details of the numerical calculations are given in the Appendix.

### A. Monopoles

We will first consider systems containing subsystems composed of a charge in the center of the spherical dielectric cavity. Figure 4 displays the reduced interaction energy  $U_{\text{int}}^{\text{red}}$  as a function of the separation variable  $R/(2a)$  for three such systems. The first system is composed of two subsystems with a charge-charge separation  $R$  [Fig. 4(a)]; the second system comprises three subsystems arranged colinearly with equal separation  $R$  between the central and its two neighboring charges [Fig. 4(b)]; and in the last system three subsystems are arranged in an equilateral triangle with charge-charge separations  $R$  [Fig. 4(c)].

Figure 4(a) shows the reduced interaction energy as function of the reduced separation between the two charges of equal (solid curves) and opposite (dashed curves) sign. In case A and with charges of the same sign and consequently  $U_{\text{int}} > 0$ , we have  $U_{\text{int}}^{\text{red}} > 1$ , i.e., the repulsive interaction becomes more repulsive, whereas with charges of the opposite sign and  $U_{\text{int}} < 0$ , we have  $U_{\text{int}}^{\text{red}} < 1$ , i.e., the attractive interaction becomes less attractive. In case B with charges of opposite sign, the reverse holds, the repulsive interaction becomes less repulsive, and the attractive interaction becomes more attractive. The changes of the interactions are between 7% and  $\approx 40\%$  at sphere contact. The qualitative influence (i) of the sign of the charges and (ii) of the relative sizes of  $\epsilon_1$  and  $\epsilon_2$  follows the leading expression given in Eq. (53). In other words, in case A with  $\epsilon_1 < \epsilon_2$  the polarization surface charges give rise to a repulsive contribution to the interaction energy and in case B with  $\epsilon_1 > \epsilon_2$  to an attractive contribution, the sign of these contributions being independent of the

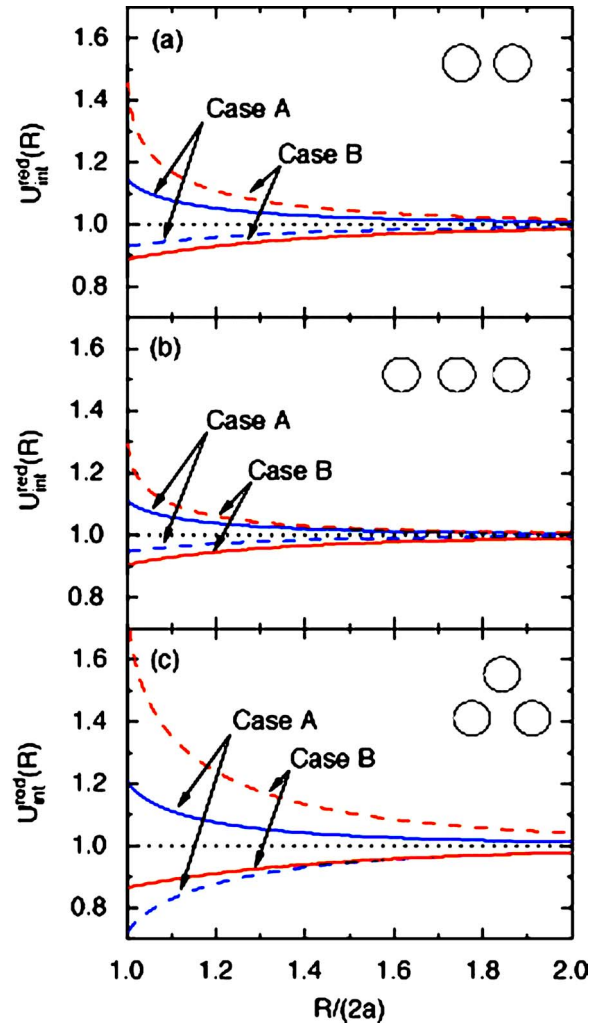


FIG. 4. (Color online) Reduced interaction energy,  $U_{\text{int}}^{\text{red}}$ , as defined by Eq. (67) as function of the reduced distance,  $R/2a$ , with  $a$  denoting the cavity radius at  $\epsilon_1=1$  and  $\epsilon_2=80$  (labeled case A) and  $\epsilon_1=80$  and  $\epsilon_2=1$  (labeled case B) for (a) two charges with same (solid curves) and opposite (dashed curves) sign; (b) three colinearly positioned charges with same (solid curves) and alternating (dashed curves) sign; and (c) three charges arranged in an equilateral triangle with same sign (solid curves) and with two positively and one negatively charged (dashed curves).

sign of the charges. Buff *et al.*<sup>20</sup> have investigated additional conditions and provided further discussion of this system, whereas the results given in Fig. 4(a), but in a slightly different representation, were presented in Fig. 5 of Ref. 19 by Allen and Hansen using a variational approach.

Figure 4(b) shows results for the three charges arranged colinearly with charges being of the same sign (solid curves) and for the central charge being the opposite of the two others (dashed curves) where the interaction energy is attractive. The qualitative dependence of  $U_{\text{int}}^{\text{red}}$  on the sign of the interaction energy and on the relative size of  $\epsilon_1$  and  $\epsilon_2$  are the same as with two charges. However, the relative influence of the polarization surface charges on  $U_{\text{int}}^{\text{red}}$  becomes smaller, due to the many-body nature of the polarization interaction. For example, with the three charges colinearly arranged, the odd moments of the polarization surface charge at the central dielectric boundary vanish due to the symmetry (the electrical fields originating from the two outer charges on the cen-

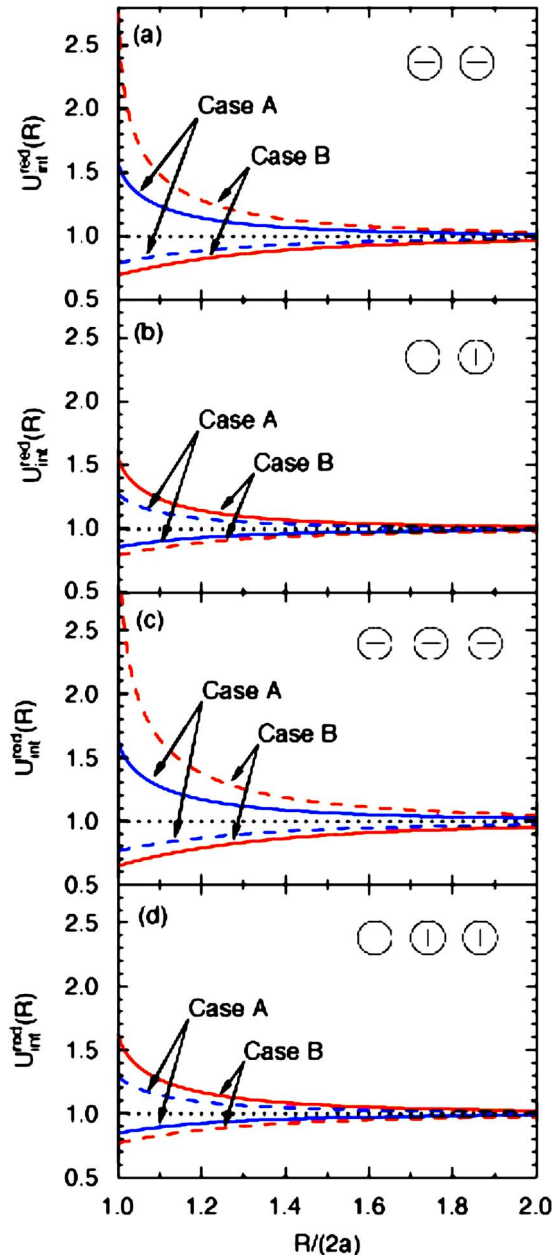


FIG. 5. (Color online) Reduced interaction energy,  $U_{\text{int}}^{\text{red}}$ , as defined by Eq. (67) as function of the reduced distance,  $R/(2a)$ , with  $a$  denoting the cavity radius at  $\epsilon_1=1$  and  $\epsilon_2=80$  (labeled case A) and  $\epsilon_1=80$  and  $\epsilon_2=1$  (labeled case B) for (a) two dipoles with dipole directions parallel to the interdipole vector with opposite (solid curves) and same (dashed curves) dipole directions; (b) two dipoles with dipole directions perpendicular to the interdipole vector with opposite (solid curves) and same (dashed curves) dipole directions; (c) three colinearly positioned dipoles with dipole directions parallel to the interdipole vector with alternating (solid curves) and same (dashed curves) dipole directions; and (d) three colinearly arranged dipoles with dipole directions perpendicular to the interdipole vector with alternating (solid curves) and same (dashed curves) dipole directions.

tral one cancel). The annihilation of the polarization surface charge multipole with  $l=1$  makes the influence of the polarization surface charges more short-ranged, an effect also visible by comparing results in panels (a) and (b) of Fig. 4.

Finally, the corresponding results when the three charges are arranged in an equilateral triangle are given in Fig. 4(c). Generally,  $U_{\text{int}}^{\text{red}}$  deviates more strongly from unity as compared to the colinear arrangement in Fig. 4(b) as well as to

the dimer in Fig. 4(a). On a qualitative level, the stronger influence of the surface polarization could be understood from the fact that the system with three charges all close to each other is electrostatically stronger interacting. A closer examination shows that the effect of the surface polarization is particularly enhanced with, say, one negative and two positive charges for both cases A and B (dashed curves). Here, the electrical fields from the two positive charges at the center of the negative charge are cooperating. We notice that attractive interaction at sphere contact is in case A with  $\epsilon_1 < \epsilon_2$  reduced by  $\approx 30\%$  and in case B with  $\epsilon_1 > \epsilon_2$  increased by  $\approx 70\%$ .

## B. Dipoles

A similar investigation of the effect of the surface polarization has been made for dipoles in spherical dielectric cavities. Figure 5 displays the reduced interaction energy  $U_{\text{int}}^{\text{red}}$  for four such systems. The first two systems comprise two dipoles with their dipole moments parallel [Fig. 5(a)] or perpendicular [Fig. 5(b)] to the interdipole vector, whereas the two last systems involve three dipoles colinearly arranged with their dipole moments parallel [Fig. 5(c)] or perpendicular [Fig. 5(d)] to the interdipole vector. In the two former systems both parallel and antiparallel orientations of the two dipoles were considered, whereas in the two last systems parallel and alternating orientations of the three dipoles are examined. Again the two conditions, case A with  $\epsilon_1 < \epsilon_2$  and case B with  $\epsilon_1 > \epsilon_2$ , have been treated.

The results given in Fig. 5 can be summarized as follows. (a) As for charges, surface polarization leads (i) in case A to that repulsive interactions become more repulsive and attractive interactions become less attractive and (ii) in case B to that repulsive interactions become less repulsive and attractive interactions become more attractive. (b) The relative change of  $U_{\text{int}}$  is larger for case B as compared to case A. (c) The effect of the surface polarization is larger when the dipoles are parallel to the interdipole direction as compared to when they are perpendicular to that direction. This could be understood from the twofold larger interaction energy for the parallel arrangement appearing for the same separation  $R$ . (d) The relative change of the interaction potential is much larger than that occurring for charges. For example, in case A and with the dielectric spheres in contact, the surface polarization increases the repulsion between two repelling charges by  $\approx 10\%$  [Fig. 4(a), solid curve], whereas the repulsion between two dipoles with the opposite direction is increased by  $\approx 50\%$  [Fig. 5(a), solid curve]. Furthermore, the magnitude of the attractive interaction between two opposite charges is reduced by  $\approx 5\%$  [Fig. 4(b), dashed curve] and that between two dipoles with the same direction is reduced by  $\approx 20\%$  [Fig. 5(a), dashed curve]. In contradiction to the case with charges, the many-body effects as expressed by  $U_{\text{int}}^{\text{red}} \neq 1$  increase with three colinear spheres as compared to 2. Here, the leading moment of the surface polarization charge of the central sphere is enhanced by the electrostatic fields of the two neighboring dipoles with same dipole directions; not annihilated as in the case with two surrounding charges of the same sign.

## VII. CONCLUSIONS

On the basis of classical equations for electrostatic fields in homogenous media and at dielectric discontinuities, a united description of the electrostatics of an arbitrary number of electrostatic multipoles, each localized in a spherical dielectric cavity, in a dielectric medium is given. Focus has been made to provide expressions of the polarization surface charge density, the electrostatic potential energy, and the electrostatic interaction for the general case, as well as in simplified cases. The correct limit of the electrostatic interaction for charges in a medium is obtained by placing the charges in a spherical dielectric cavity, solving the equations describing the electrostatics, and then taking the limit of zero cavity radii. Interacting electrostatic multipoles in dielectric spheres immersed in a medium with a higher (lower) relative dielectric permittivity experience a repulsive (attractive) potential term that increases in magnitude at reduced multipole separation, originating from the polarization surface charges appearing at the dielectric interfaces.

## ACKNOWLEDGMENTS

Valuable discussions with Phil Attard, Bengt Jönsson, Gunnar Karlström, and Jurij Reščič as well as financial support by the Swedish Research Council (VR) through the Linnaeus Center of Excellence on Organizing Molecular Matter (OMM) are gratefully acknowledged.

## APPENDIX: COMPUTATIONAL ASPECTS

In a numerical solution, the expansion of the surface charge density,  $\sigma(\Omega)$ , in spherical harmonics,  $C_{lm}$ , given by Eq. (8) needs to be truncated. The  $l$  index of the highest surface charge multipole moment  $\sigma_{lm}$  included is denoted by  $l_{\max}$ . These multipole moments were solved iteratively according to Eq. (31) and the total electrostatic energy and the interaction energy were evaluated using Eqs. (32)–(35) employing a FORTRAN 90 computer program.<sup>32</sup> Faster algorithms were implemented for systems (i) possessing axial symmetry and/or (ii) carrying charges only, using simpler expressions.

The truncation error and the computational time will be given for solving a system involving two subsystems, each being composed of a unit charge at the center of a dielectric sphere, at the separation  $R/(2a)=1.001$  with  $a=1$  and with  $\epsilon_1=1$  and  $\epsilon_2=80$ . Hence, the surface-to-surface separation between the two spheres is 0.1% of the diameter of the sphere. The convergence in  $l_{\max}$  becomes quickly faster at larger separation. Throughout, the iteration of the multipole moments were terminated when the change in  $U$  between two iterations were below  $10^{-9}$ .

Figure 6(a) shows the total electrostatic energy  $U$  given by Eqs. (32) and (33) and the reduced interaction energy  $U_{\text{int}}^{\text{red}}$  given by Eq. (67) relative to their values at  $l_{\max}=100$  as a function of  $l_{\max}$ . If we, for simplicity, regard the values at  $l_{\max}=100$  as the exact ones, the ordinate provides the truncation errors for a given value of  $l_{\max}$ . First, and as expected, the truncation errors decrease with increasing  $l_{\max}$ . Furthermore, the truncation error of  $U_{\text{int}}^{\text{red}}$  is  $\approx 100$  times larger than that of  $U$ , the reason being that  $|U_{\text{int}}| \approx 0.01|U|$  due to the canceling effect in Eq. (34) when forming the interaction

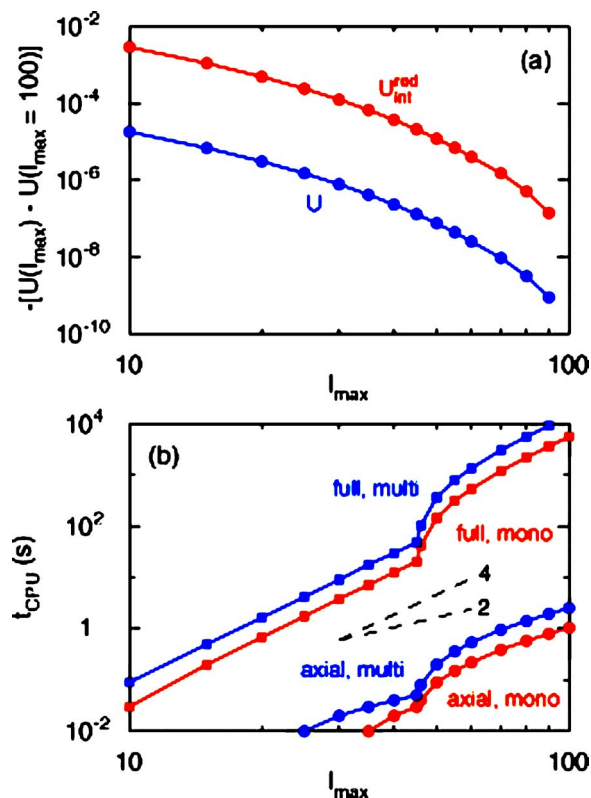


FIG. 6. (Color online) (a) Total electrostatic energy,  $U$ , and reduced interaction energy,  $U_{\text{int}}^{\text{red}}$ , and (b) the CPU time,  $t_{\text{CPU}}$ , as a function of the truncation of the spherical harmonic expansion of the polarization surface charge density,  $l_{\max}$ , for a system composed of two subsystems, each composed of a unit charge localized in a spherical dielectric cavity with the relative permittivity  $\epsilon_1=1$  in a medium characterized by  $\epsilon_2=80$  at a separation  $R/(2a)=1.001$ , where  $a=1$  is the cavity radius. In (a), the values are given with respect to those for  $l_{\max}=100$ . In (b), data are given for full treatment (full) and axial symmetry (axial), as well as for general multipoles (multi) and charges (mono). The dashed lines show the slopes 2 and 4.

energy. In the main calculations,  $l_{\max}=60$  has been adopted; thus providing five significant figures of  $U_{\text{int}}^{\text{red}}$  at the shortest separation  $R/(2a)=1.001$  considered. As mentioned, the truncation error of  $U_{\text{int}}^{\text{red}}$  becomes rapidly much smaller at increasing  $R$ .

The CPU time  $t_{\text{CPU}}$  for these calculations is provided in Fig. 6(b). It is observed that a reduction from a full treatment to algorithms taking into account axial symmetry decreases  $t_{\text{CPU}}$  by two to four orders of magnitude, the reduction being dependent on  $l_{\max}$ . The effect of having only charges instead of general multipoles reduces  $t_{\text{CPU}}$  by a factor of 2. The number of operations for the iterative solution and interaction calculations both scales roughly as  $n_{\text{op}} \propto n_{\text{coeff}}^2$ , where the number of expansion coefficients  $\sigma_{lm}$  per cavity is  $n_{\text{coeff}} = (1+l_{\max})^{\gamma'}$  with  $\gamma'=2$  with a full treatment and  $\gamma'=1$  with axial symmetry. Hence, theoretically we have the estimate  $n_{\text{op}} \propto (1+l_{\max})^{\gamma} \approx l_{\max}^{\gamma}$  with  $\gamma=4$  and 2, respectively. Figure 6(b) shows that  $t_{\text{CPU}} \propto l_{\max}^{\gamma}$  with  $\gamma \approx 4$  with a full treatment and  $\gamma \approx 2$  with axial symmetry, consistent with this estimate. The increased slope appearing after  $l_{\max}=45$  originates from the use of an increased precision in the evaluation of the  $f$  function given by Eq. (29) when  $l > 45$ . However, at  $l_{\max} \gg 45$  the power law dependence with the original exponents resumes.

- <sup>1</sup>C. J. F. Böttcher, *Theory of Electric Polarization* (Elsevier, Amsterdam, 1973).
- <sup>2</sup>J. D. Jackson, *Classical Electrodynamics* (Wiley, New York, 1975).
- <sup>3</sup>D. F. Evans and H. Wennerström, *The Colloidal Domain Where Physics, Chemistry, Biology, and Technology Meet* (VCH, New York, 1994).
- <sup>4</sup>T. L. Hill, *Statistical Mechanics* (Dover, New York, 1987).
- <sup>5</sup>S. Gavryushov and P. Linse, *J. Phys. Chem. B* **110**, 10878 (2006).
- <sup>6</sup>B. Hess, C. Holm, and N. van der Vegt, *Phys. Rev. Lett.* **96**, 147801 (2006).
- <sup>7</sup>P. J. Lenart, A. Jusufi, and A. Z. Panagiotopoulos, *J. Chem. Phys.* **126**, 044509 (2007).
- <sup>8</sup>B. Jönsson and H. Wennerström, in *Electrostatic Effects in Soft Matter and Biophysics*, edited by C. Holm, P. Kékicheff, and R. Podgornik (Kluwer Academic, London, 2001), Vol. 56, p. 171.
- <sup>9</sup>V. Vlachy, *Annu. Rev. Phys. Chem.* **50**, 145 (1999).
- <sup>10</sup>J.-P. Hansen and H. Löwen, *Annu. Rev. Phys. Chem.* **51**, 209 (2000).
- <sup>11</sup>L. Belloni, *J. Phys.: Condens. Matter* **12**, R549 (2000).
- <sup>12</sup>L. B. Bhuiyan, V. Vlachy, and C. W. Outhwaite, *Int. Rev. Phys. Chem.* **21**, 1 (2002).
- <sup>13</sup>P. Linse, in *Advanced Computer Simulation Methods in Soft Matter Sciences*, edited by C. Holm and K. Kremer (Springer, New York, 2005), Vol. 185, p. 111.
- <sup>14</sup>P. Linse, *J. Phys. Chem.* **90**, 6821 (1986).
- <sup>15</sup>G. Iversen, Y. I. Kharkats, and J. Ulstrup, *Mol. Phys.* **94**, 297 (1998).
- <sup>16</sup>R. Messina, *J. Chem. Phys.* **117**, 11062 (2002).
- <sup>17</sup>D. K. Ross, *SIAM J. Appl. Math.* **29**, 699 (1975).
- <sup>18</sup>Y. Nakajima and T. Sato, *J. Electrostat.* **45**, 213 (1999).
- <sup>19</sup>R. Allen and J.-P. Hansen, *J. Phys.: Condens. Matter* **14**, 11981 (2002).
- <sup>20</sup>F. P. Buff, N. S. Goel, and J. R. Clay, *J. Chem. Phys.* **63**, 1367 (1975).
- <sup>21</sup>W. D. Hall and K. V. Beard, *Pure Appl. Geophys.* **113**, 515 (1975).
- <sup>22</sup>É. D. German and Y. I. Kharkats, *Russ. Chem. Bull.* **34**, 1634 (1985).
- <sup>23</sup>M. Born, *Z. Phys.* **1**, 45 (1920).
- <sup>24</sup>R. P. Bell, *Trans. Faraday Soc.* **27**, 797 (1931).
- <sup>25</sup>L. Onsager, *J. Am. Chem. Soc.* **58**, 1486 (1936).
- <sup>26</sup>R. Allen, J.-P. Hansen, and S. Melchionna, *Phys. Chem. Chem. Phys.* **3**, 4177 (2001).
- <sup>27</sup>P. Attard, *J. Chem. Phys.* **119**, 1365 (2003).
- <sup>28</sup>J. Rescic and P. Linse, *J. Chem. Phys.* (submitted).
- <sup>29</sup>D. M. Brink and G. R. Satchler, *Angular Momentum* (Clarendon, Oxford, 1968).
- <sup>30</sup>S. Levine and H. E. Wrigley, *Discuss. Faraday Soc.* **24**, 43 (1957).
- <sup>31</sup>P. S. Ramanathan and H. L. Friedman, *J. Chem. Phys.* **54**, 1086 (1971).
- <sup>32</sup>The computer program DIELEC used in this work and written in FORTRAN 90 is available from the author. Exploring test computations can also be made from the web portal [www.fkem1.lu.se/sm](http://www.fkem1.lu.se/sm).